Table S1. List of strong hits in *Brucella neotomae* high throughput, host cell anti-cytotoxicity screen analyzed in secondary assays.

HTS z-score	Compounds	Category	Function	Final Concentration	Secondary Screening z-score	Percent Growth Inhibition
-13.1	Indirubin-3'-monoxime	Kianse inhibitor	CDK/GSK-3β inhibitor	10 μg/mL	-10.40	132.2 ± 4.1
-11.3	Mitoxantrone 2HCl	antimicrobial	chemotherapeutic	4 μg/mL	-10.40	142.8 ± 3.0
-7.3	BX912	Kinase Inhibitor	PDK1 inhibitor	4 μM	-10.34	101.0 ± 0.2
-10.3	IKK Inhibitor VII	Kinase Inhibitor	IκB kinase (IKK) inhibitor	20 μM	-10.31	116.4 ± 1.1
-9.3	DMAB-anabaseine dihydrochlori	GPCR	Nicotinic (α7) Receptor Agonist	20 μM	-10.31	107.0 ± 8.1
-7.2	ZM 226600	Ion channel modul	Kir6 (KATP) channel opener	20 μM	-10.16	104.6 ± 10.9
-7.7	Arcyriaflavin A	Kinase Inhibitor	CDK4/cyclin D1 inhibitor	20 μM	-10.02	95.6 ± 5.8
-10.9	CYT387	Kinase Inhibitor	JAK inhibitor	4 μM	-10.00	95.5 ± 0.1
-7.3	Rhodblock 6	Kinase Inhibitor	Rho kinase inhibitor	20 μM	-9.99	98.0 ± 7.8
-7.4	NS8593 hydrochloride	Ion channel modul	KCa2 (SK) channel negative mo	20 μM	-9.78	94.9 ± 9.7
-7.1	N6-Cyclohexyladenosine	GPCR	A1 adenosine receptor agonist	20 μM	-9.60	91.2 ± 2.3
-7.0	SDZ WAG 994	GPCR	Adenosine A1 receptor agonist	20 μM	-9.57	91.1 ± 7.2
-7.1	MDL 73005EF hydrochloride	GPCR	SR-1A partial agonist	20 μM	-9.49	90.1 ± 11.2
-7.2	(±)-5'-Chloro-5'-deoxy-ENBA	GPCR	Adenosine A1 receptor agonist	20 μM	-9.34	88.6 ± 3.7
-7.5	Esomeprazole magnesium dihydr	proton pump inhib	proton pump inhibitor	20 μM	-9.19	86.9 ± 2.1
-7.3	ABT 724 trihydrochloride	GPCR	D4DR (dopamine D4 receptor) a	20 μM	-8.73	82.1 ± 7.9
-7.4	Flutamide	GPCR	Androgen Receptor Inhibitor	20 μM	-8.29	77.4 ± 4.3
-8.5	Pinacidil	Ion channel modul	ATP-sensitive potassium channe	20 μM	-7.97	74.0 ± 12.5
-7.5	SP-600125	Kinase Inhibitor	JNK Inhibitor	10 μg/mL	-7.94	73.8 ± 4.5
-8.5	Buspirone hydrochloride	GPCR	5-HT1A partial agonist	4 μg/mL	-7.76	71.9 ± 6.5
-7.5	8-Cyclopentyl-1,3-dimethylxanth	GPCR	A1 adenosine receptor antagonis	20 μM	-7.65	70.7 ± 12.3
-11.1	LY-83583	other	soluble guanylate cyclase inhibi	10 μg/mL	-7.64	70.6 ± 14.3
-8.1	Doxazosin mesylate	GPCR	α1 antagonist	4 μg/mL	-7.52	69.4 ± 7.6
-9.1	KI20227	Kinase Inhibitor	CSF1R inhibitor	4 μM	-7.33	67.3 ± 1.9
-7.2	Crinamine	other	HIF1a inhibitor	20 μM	-5.95	52.8 ± 16.6
-7.8	AG 555	Kinase Inhibitor	EGFR inhibitor	20 μM	-4.75	40.1 ± 7.5
-8.0	RN 1747	Ion channel modul	TRPV4 agonist	20 μM	-4.46	37.1 ± 10.4
-7.0	Dantrolene	Ion channel modul	Ca2+ ions inhibitor	10 μg/mL	-4.08	33.1 ± 2.2
-7.1	GW 441756	Kinase Inhibitor	TrkA inhibitor	20 μM	-3.87	30.8 ± 0.8
-8.0	SU-4312	Kinase Inhibitor	EGFR and c-Src tyrosine kinase	10 μg/mL	-3.86	31.1 ± 6.1
-7.0	Ro 90-7501	other	inhibitor of Aß42 fibril formatio	20 μM	-3.74	29.6 ± 6.0
-7.2	Tyrphostin AG 835	Kinase Inhibitor	Casein kinase II inhibitor	20 μM	-3.64	28.4 ± 12.3
-8.7	Rabeprazole sodium	proton pump inhib	proton pump inhibitor	4 μg/mL	-3.63	28.3 ± 10.5
-7.6	Pantoprazole	proton pump inhib	proton pump inhibitor	4 μg/mL	-3.59	28.0 ± 2.5
-9.1	Alfluzosin	GPCR	α1 adrenoceptor antagonist	4 μg/mL	-3.59	27.9 ± 2.1
-8.6	Cilostazol	other	PDE3 inhibitor	4 μg/mL	-3.42	26.2 ± 1.2
-8.5	Tanshinone IIA	other		10 μg/mL	-3.38	25.7 ± 16.6
-7.1	GW-5074	Kinase Inhibitor	Raf Inhibitor	10 μg/mL	-3.28	24.7 ± 23.5
-7.7	AG 490	Kinase Inhibitor	EGFR inhibitor	20 μM	-3.14	23.2 ± 1.6
-7.1	R(-)-2,10,11-Trihydroxyaporphin	GPCR	D2 dopamine receptor agonist	20 μM	-2.46	16.0 ± 2.6
-11.6	Epigallocatechin gallate	other		20 μM	-2.29	14.3 ± 9.5
-7.5	Tyrphostin B44, (+) enantiomer	Kinase Inhibitor	EGFR kinase inhibitor	20 μM	-2.25	13.8 ± 3.4
-7.1	Phenserine	other	AChE inhibitor	20 μM	-2.15	12.8 ± 12.5
-7.3	GF 109203X	Kinase Inhibitor	PKC inhibitor	20 μM	-2.08	12.0 ± 19.5
-7.1	Nafamostat mesylate	other	serine proteass inhibitor, anticoa	10 μg/mL	-1.81	9.2 ± 8.6
-7.2	SR 11302	other	AP-1 inhibition-specific retinoic	20 μM	-1.21	2.8 ± 11.7
-7.4	Cortisone	steroid	steroid	20 μM	-0.55	-4.2 ± 13.3
-7.0	NU6027	Kinase Inhibitor	ATR/CDK Inhibitor	20 μM	-0.17	-8.1 ± 4.2
-7.1	Nifedipine	Ion channel modul	Ca2+ ions inhibitor	4 μg/mL	3.52	-47.0 ± 8.6

*shading indicates compounds that were further studied in this manuscript

Table S2. List of siRNA nucleotides used in hit target and autophagy protein knockdown experiments.

siRNA	Sequences (5'-3') Sense	Reference	Identifier
ATG5si	1. CUCUCUAUCAGGAUGAGAUAACUGA 2. CUUGGAACAUCACAGUACAUUUCAA	This paper	N/A
ATG12si	1. ACCAAGAAGUUGGAACUCUAUAUGA 2. GUUGUUUAUUUAUGUGAAUCAGUCC	This paper	N/A
LC3si	1. AGCGAGCUCAUCAAGAUAAUCAGAC 2. AUGAGCGAGCUCAUCAAGAUAAUCA	This paper	N/A
p62si	1. AGGUUGACAUUGAUGUGGAACAUGG 2. CUGACAGAGCAAAUGAAAAAGAUAG	This paper	N/A
CDK1si	1. AGAAAAUUGGAGAAGGUACUUACGG 2. GACUUGGACAAUCAGAUUAAGAAGA	This paper	N/A
CDK4si	1. CAGAGAACAUUCUAGUGACAAGUAA 2. CUGAAGCCAGAGAACAUUCUAGUGA	This paper	N/A
CSF1Rsi	1. GGCAUCUGGCUUAAGGUGAAUCGAG 2. GGAAUAAUCUGACCUUUGAGCUCAC	This paper	N/A
JAK1si	1. GAGGUGACUUUCUAUCUGUUGGACA 2. AAACAUUGAAUAAAUCCAUCAGACA	This paper	N/A
Rab7si	GCCUCCGCAGAAAGCUGCAGUUGUU	ThermoFisher	MSS276705
Negative control DsiRNA (NTsi)	CGUUAAUCGCGUAUAAUACGCGUAT	IDT	#51-01-14-03

Table S3. List of oligonucleotide primer sequences used for analysis of qPCR-based mRNA expression analysis in siRNA-knockdown experiments.

Target genes	Primer Sequences (5'-3')	Reference	Genbank accession for gene target
CDK1	CCGGTTGACATCTGGAGTATAG/ ATCCTGAAGAGCTGGTCAATC	This paper	NM_007659
CDK4	TTTCTAAGCGGCCTGGATTT/ GCTTGACGGTCCCATTACTT	This paper	NM_009870
CSF1R	CTGGGACAGCACGAGAATATAG/ TCCTTCGGAGAAAGTTGAGATG	This paper	NM_001037859
JAK1	CCTCATGAACCACCTCAAGAA/ GCTACGAGCAGATTGGAGATT	This paper	NM_146145
β-actin	GTGGGAATGGGTCAGAAGG/ GCTCATTGTAGAAGGTGTGG	Kang & Kirby (2019)	NM_007393.5

Kang YS, Brown DA, Kirby JE. 2019. *Brucella neotomae* recapitulates attributes of zoonotic human disease in a murine infection model. Infect Immun. 87: pii: e00255-18.

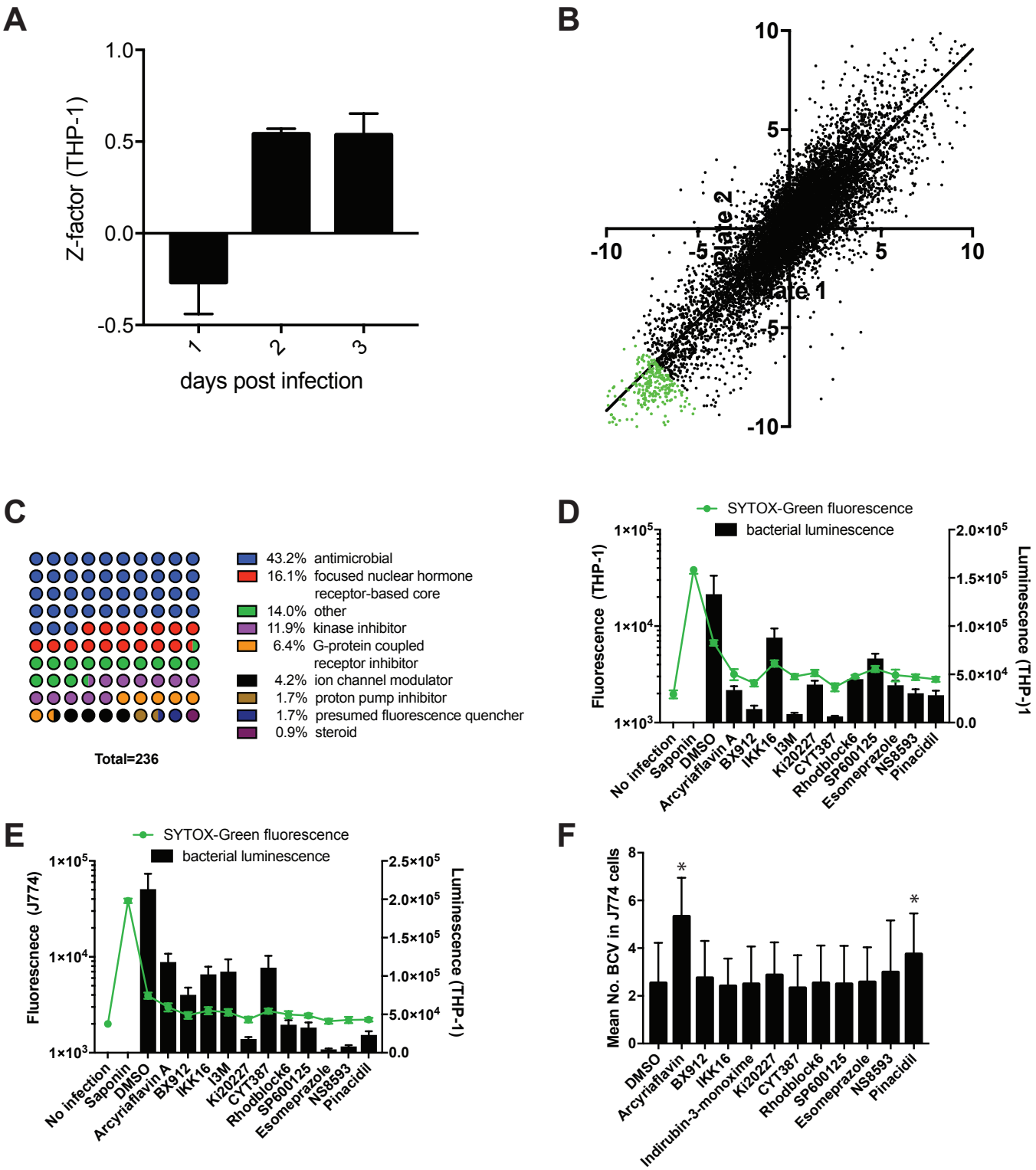
A
Z-factor (THP-1)
1.0
0.5
0.0
-0.5
1
2
3
days post infection
B
10
5
-5
-10
-10
-5
5
10
C
43.2% antimicrobial
16.1% focused nuclear hormone receptor-based core
14.0% other
11.9% kinase inhibitor
6.4% G-protein coupled receptor inhibitor
4.2% ion channel modulator
1.7% proton pump inhibitor
1.7% presumed fluorescence quencher
0.9% steroid
Total=236
D
SYTOX-Green fluorescence
bacterial luminescence
Fluorescence (THP-1)
Luminescence (THP-1)
1×10^5
1×10^4
1×10^3
2.0×10^5
1.5×10^5
1.0×10^5
5.0×10^4
0.0
No infection
Saponin
DMSO
Arcyriaflavin A
BX912
IKK16
I3M
Ki20227
CYT387
Rhodblock6
SP600125
Esomeprazole
NS8593
Pinacidil
E
SYTOX-Green fluorescence
bacterial luminescence
Fluorescnece (J774)
Luminescence (THP-1)
1×10^5
1×10^4
1×10^3
2.5×10^5
2.0×10^5
1.5×10^5
1.0×10^5
5.0×10^4
0.0
No infection
Saponin
DMSO
Arcyriaflavin A
BX912
IKK16
I3M
Ki20227
CYT387
Rhodblock6
SP600125
Esomeprazole
NS8593
Pinacidil
F
Mean No. BCV in J774 cells
8
6
4
2
0
*
*
DMSO
Arcyriaflavin
BX912
IKK16
Indirubin-3-monoxime
Ki20227
CYT387
Rhodblock6
SP600125
Esomeprazole
NS8593
Pinacidil

Figure S1. High throughput screening assay characteristics. (A) Bn infection of THP-1 cells were allowed to proceed for indicated time points in the presence of SYTOX Green to provide a real-time indicator of eukaryotic cell toxicity. Positive control wells contained antibiotic to inhibit intracellular bacterial growth. Negative controls wells contained corresponding amount of DMSO. Z-factor was maximal two days post infection. Bar height and error bars reflect the mean and S.D. for Z-factor determinations from three separate experiments, 20 replicate test wells per condition per experiment. **(B)** XY-scatter plot of z-score replicates for each tested compound, the z-score for the first replicate indicated by X-axis coordinate and the second replicate by the Y-axis coordinate for each data point. $R^2 = 0.83$. Zero values reflect control levels of cytotoxicity induced by intracellular growth 48 hours post infection. Negative z-scores reflect inhibition of eukaryotic cell toxicity reflected in negative fluorescence compared with untreated control wells. Green colored data represent strong hits, which were considered for further analysis. **(C)** General categorization of screening hits from known bioactive libraries. Tally was performed after removing compounds that were duplicated in the multiple known bioactive libraries tested. **(D)** Bacterial luminescence and THP-1 host cell cytotoxicity. Bacterial luminescence as a measure of intracellular replication and SYTOX Green fluorescence as a measure of host cell cytotoxicity were measured contemporaneously 48 h post infection in the same assays wells in the presence of absence of compounds at same concentrations used in Fig. 1A. 0.1% saponin, a detergent, was used a positive control for host cell cytotoxicity that lyses host cells and prevents bacterial growth. Inhibitors decreased both intracellular growth and host cell cytotoxicity. Data are the mean and standard deviation for sextuplicate test wells. Inhibitors significantly decreased ($P < 0.0001$, post hoc Dunnett's multiple comparison tests) both intracellular growth and host cell cytotoxicity for all conditions compared with DMSO infected control (except for saponin lysis which caused significantly greater fluorescence). **(E)** Bacterial luminescence and J774A.1 host cell cytotoxicity. Bacterial luminescence as a measure of intracellular replication and SYTOX-Green fluorescence as a measure of host cell cytotoxicity were measured contemporaneously 48 h post infection in the same assays wells in the presence of absence of compounds at same concentrations used in Fig. 1A. Data are the mean and standard deviation for sextuplicate test wells. 0.1% saponin was used a positive control for host cell cytotoxicity. Inhibitors significantly decreased ($P < 0.05$, post hoc Dunnett's multiple comparison tests) both intracellular growth and host cell cytotoxicity for all conditions compared with DMSO infected control (except for saponin lysis which caused significantly greater fluorescence). The magnitude of host cell cytotoxicity resulting from intracellular infection of J774A.1 cells was lower than for THP-1 cells. Correspondingly, the magnitude of cytotoxicity suppression by inhibitors was also lower for J774A.1 cells. **(F)** At 4 h post infection, the mean number and S.D. of intracellular Bn in infected J774A.1 cells was determined by confocal microscopy; 50 host cells were scored per condition. There were no significant difference between uptake in inhibitor treated host cells, with the exception of a significant increase (*) in uptake during treatment with arcyriaflavin A and pinacidil in post hoc comparisons with DMSO control.

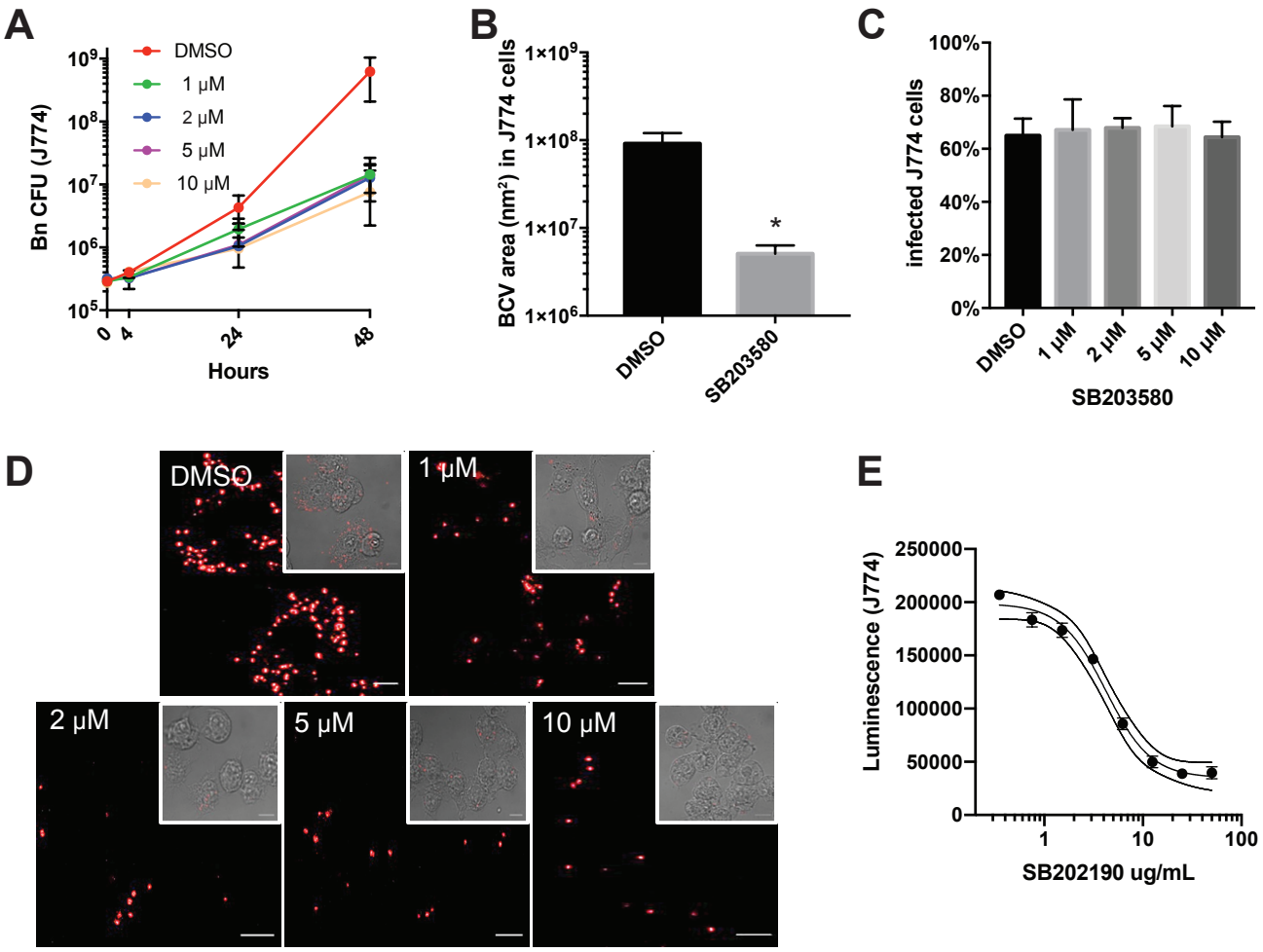

Figure S2. MAPK p38 is induced by and modulates intracellular infection. (A) Effect of p38 MAPK inhibition by SB203580 on intracellular growth of *B. neotomae*. J774A.1 cells were treated with SB203580 at indicated concentrations and infected with *B. neotomae* (Bn). Intracellular CFUs were determined at 0, 4, 24, and 48 h post infection. Data presented are the mean ± SD from two independent experiments. **(B)** Mean ± S.D. of the area occupied by BCV 48 h post infection in ten infected J774A.1 host cells scored per condition from confocal microscopy images. P = 0.001 for comparison with DMSO control. **(C)** At 24 h post infection, the mean percentage ± S.D. of J774A.1 cells infected with any *B. neotomae* in the presence of indicated concentration of SB203580 or DMSO control was determined by confocal microscopy; >100 host cells were scored per condition over 3 independent experiments. There were no significant differences in uptake between conditions ($P = 0.9$). **(D)** J774A.1 cells were similarly treated and infected with *B. neotomae* expressing tdTomato at an MOI of 1. Representative confocal micrographs 24 h post infection are shown. **(E)** Effect of SB202190, an alternative p38 MAPK inhibitor on intracellular growth (luminescence) in J774A.1 host cells. Dose-response analysis (solid line) indicates IC_{50} of ~4 μg/mL determined from a non-linear four parameter regression with 95% confidence interval shown as dotted lines.

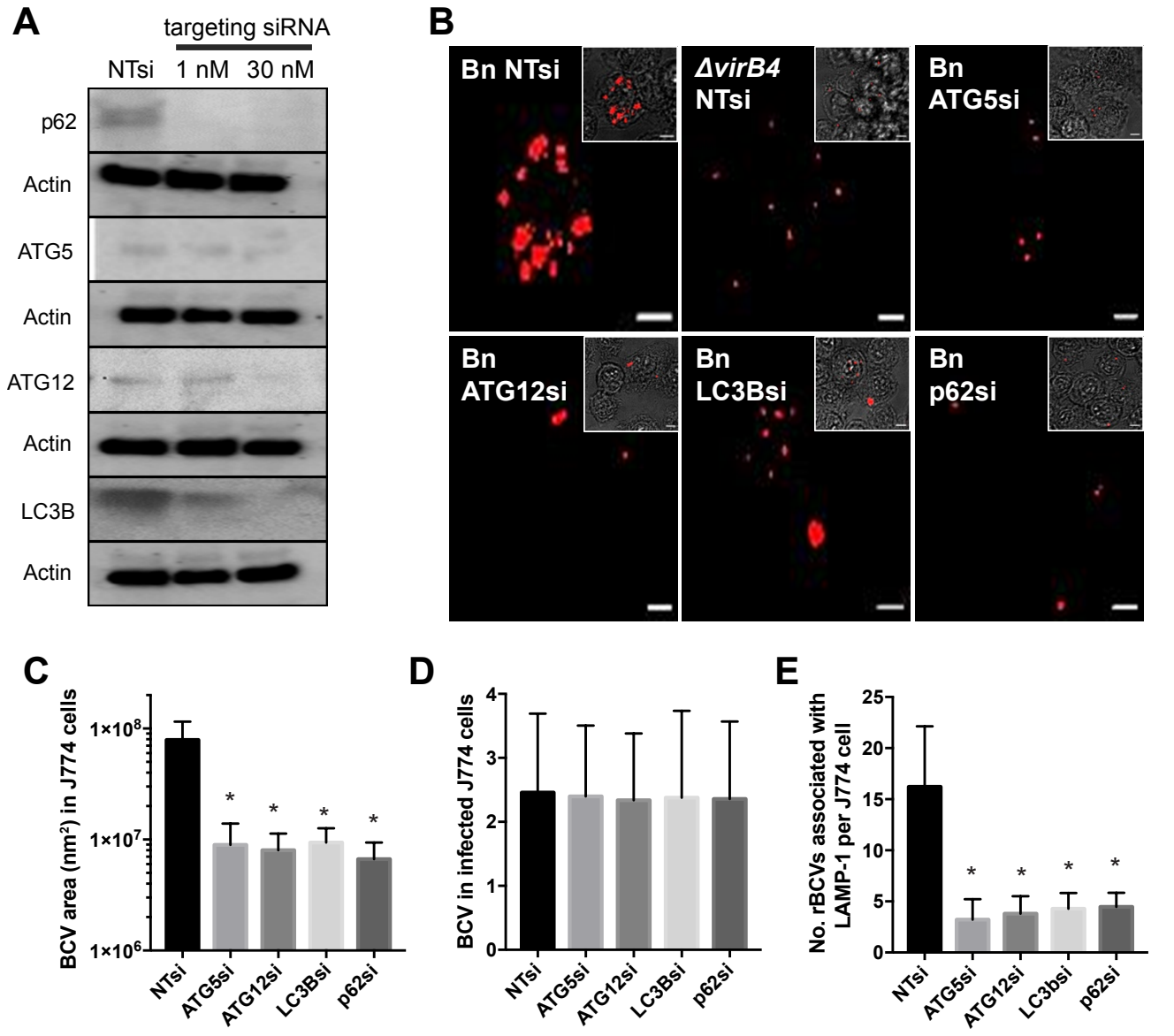

Figure S3. Autophagy-related proteins are required for the intracellular growth of Bn in J774A.1 macrophages. (A) Western blot analysis of the expression of autophagy-related protein and β-actin loading control in J774A.1 cells transfected with corresponding targeting or non-targeting siRNA and detection with cognate antibodies. ATG5 and ATG12 antibodies, respectively, detect the conjugated form of ATG5-ATG12, which runs at ~56kDa. NTsi was transfected at 50 nM. **(B)** The intracellular replication of tdTomato reporter-labeled Bn WT or *ΔvirB4* strain in J774A host cells transfected with indicated siRNA. Infections were at an MOI 1, and images were acquired 24 h post infection. Size bars: 5 μm. **(C)** Mean ± S.D. of the area occupied by BCV in confocal images of 10 infected host cells scored per condition 48 h post infection. $P = 0.001$ for each pairwise post hoc comparison with NTsi control. **(D)** At 4 hours post infection, the mean number ± S.D. of intracellular Bn in infected J774A.1 cells was determined by confocal microscopy; 50 host cells were scored per condition. There were no significant differences in uptake between siRNA-treated host cells compared to NTsi control ($P > 0.9$ for all pairwise post hoc comparisons). **(E)** Quantification of the mean number ± S.D of rBCV associated with LAMP-1 in infected J774A.1 cells 48 h post infection. rBCV are defined by BCV > 2μM. 50 infected host cells scored per condition. $P \leq 0.001$ for each pairwise post hoc comparison with NTsi control. In figure panels, * designates significant difference in post hoc comparisons with NTsi control.

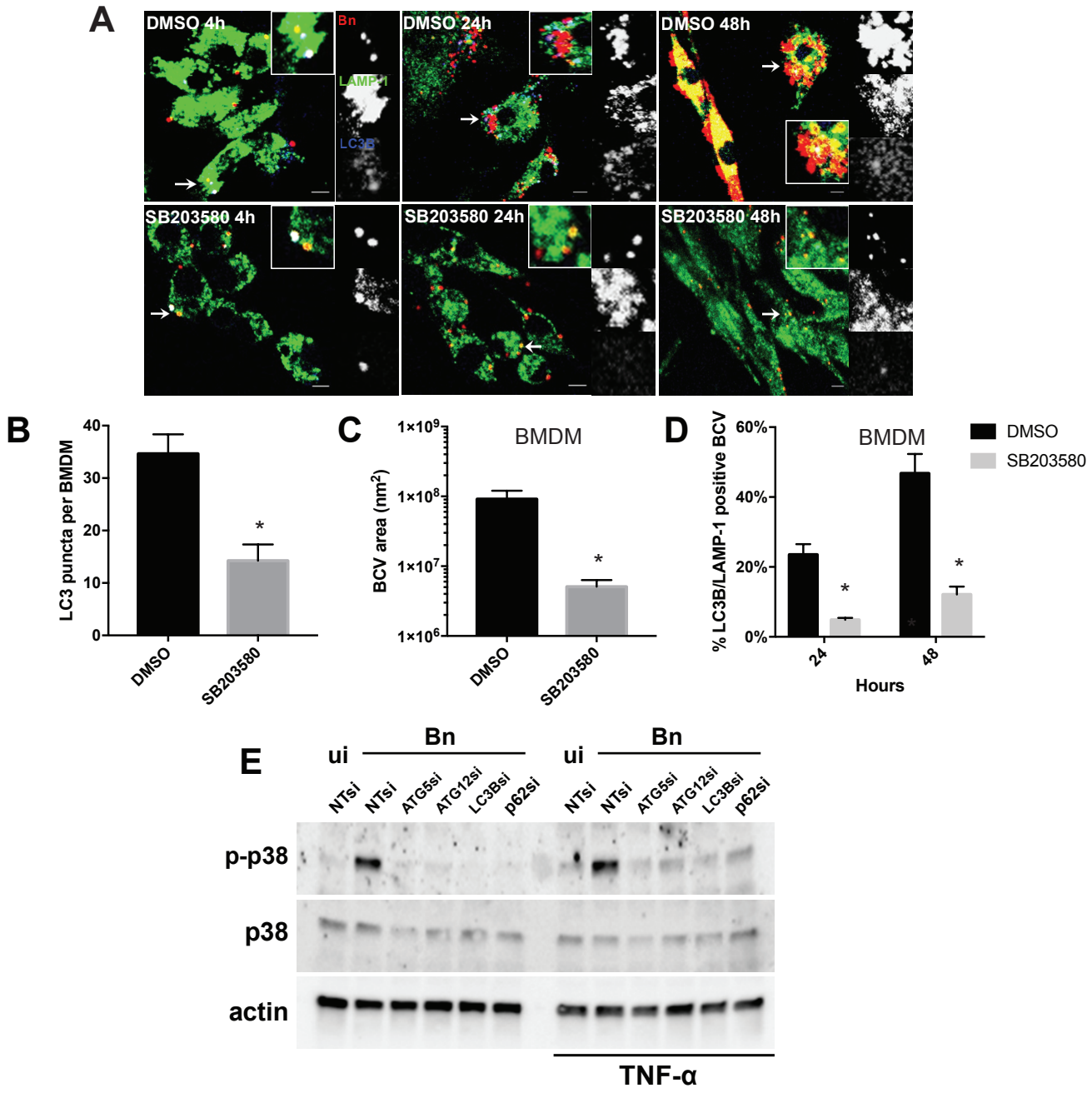

Figure S4. Linkage between p38 and autophagy pathways. (A) Colocalization of LC3B (blue), LAMP-1 (green), and Bn (red) in bone marrow-derived macrophages (BMDM) isolated from BALB/c mice) treated with DMSO or 10 μM of SB203580. Arrows highlight colocalization of BCV with LC3B and LAMP-1 highlighted in insets. Scale bar: 5 μm. **(B)** The mean number ± SD of LC3 puncta from fifty infected BMDM per condition four hours post infection. **(C)** The mean ± S.D. of the area occupied by BCV 48 h post infection in ten infected BMDM scored per condition from confocal microscopy images. $P < 0.0001$ for comparison with DMSO control. **(D)** Percent colocalization of BCV with both LC3B and LAMP-1 in BMDM 24 and 48 h post-infection. Data shown are the mean ± SD from three independent experiments with > 75 BCV scored per condition per experiment. In figure panels, * designates significant difference in comparisons with DMSO control (Student's t-test, $P < 0.05$). **(E)** Autophagy pathway siRNA knockowns selectively inhibit p38 phorphorylation induced by Bn but not by TNF-α in J774A.1 host cells. Western blots performed on lysates of either infected (Bn) or uninfected (ui) J774A.1 cells transfected with indicated siRNA and/or treated with 100 ng/mL TNF-α. Infections were for 48 h. TNF-α induced a modest increase in p38 phophorylation in uninfected host cells and in siRNA treated host cells infected with Bn.

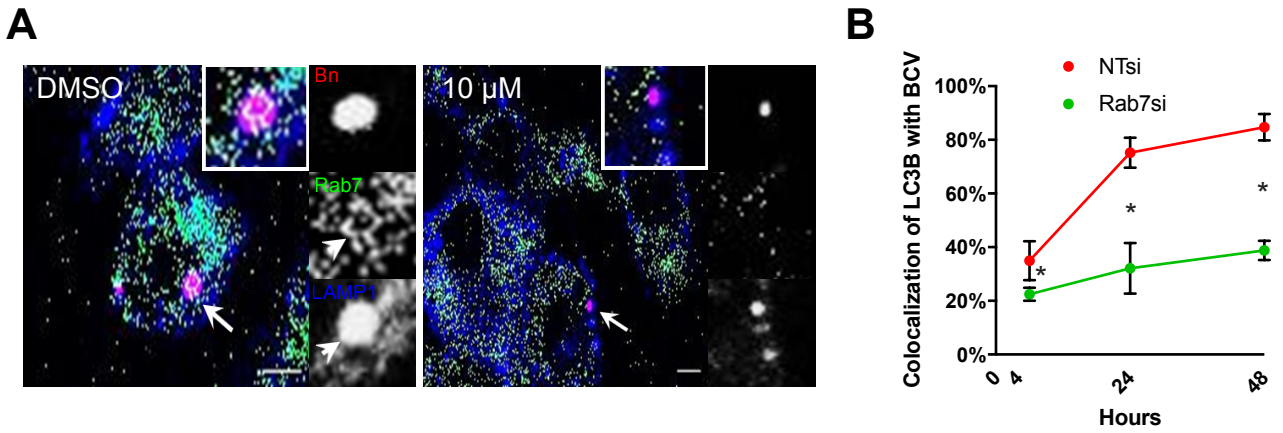

Figure S5. Rab7 and p38 are required for BCV maturation in J774A.1 host cells. (A) SB203580 treatment inhibited colocalization of Rab7 (green) with BCV (red). Shown are representative confocal micrographs of J774A.1 cells 6 h post infection. Arrows point respectively under control conditions to an example of a LAMP-1::mTurquoise2-positive BCV to which there is significant Rab7 recruitment, and with 10 µM SB203580 treatment to a BCV that is LAMP-1::mTurquoise2 positive and Rab7 negative. Size bar: 5 µm. **(B)** Effect of 50 nM Rab7si transfection on LC3B colocalization with BCV in J774A.1 host cells enumerated from confocal images. Each data point represents mean percent colocalization ± SD from four independent experiments scoring at least 50 representative BCV per condition per experiment. In figure panels, * designates significant difference in comparisons with NTsi control.